Hyperfine Interact (2017) 238:39
DOI 10.1007/s10751-017-1415-9

Chemical Information revealed by Mössbauer spectroscopy and DFT calculations

Satoru Nakashima[1,2]

Abstract Mixed-valence state of binuclear metallocene derivatives and spin-crossover (SCO) phenomena of the assembled Fe(II) complexes have been studied by using Mössbauer spectroscopy. The understanding of the results obtained by Mössbauer spectra is well supported by means of X-ray structural analysis and density functional theory (DFT) calculation. Benchmark study of relativisitic DFT calculation by using Mössbauer isomer shifts of Eu, Np complexes reveals the validity of the calculation. Such study sheds light on the bonding character of 4f and 5f electron. These results are reviewed.

Keywords Mössbauer isomer shift · Density functional theory · Mixed-valence state · Spin crossover · Benchmark study · X-ray structural analysis · f-block element

1 Introduction

Mössbauer spectroscopy is a powerful tool to investigate materials science such as magnetism and chemistry of coordination compounds and iron oxides [1]. Hyperfine interactions are useful for such research. Isomer shift (IS) is determined by electron density of absorber atom at nuclear position. The IS value reflects the oxidation state and bonding

This article is part of the Topical Collection on *Proceedings of the 15th Latin American Conference on the Applications of the Mössbauer Effect (LACAME 2016), 13–18 November 2016, Panama City, Panama*
Edited by Juan A. Jaén

✉ Satoru Nakashima
snaka@hiroshima-u.ac.jp

[1] Natural Science Center for Basic Research and Development, Hiroshima University, 1-4-2, Kagamiyama, Higashi-Hiroshima, 739-8526, Japan

[2] Graduate School of Science, Hiroshima University, 1-3-1, Kagamiyama, Higashi-Hiroshima, 739-8526, Japan

Published online: 21 February 2017

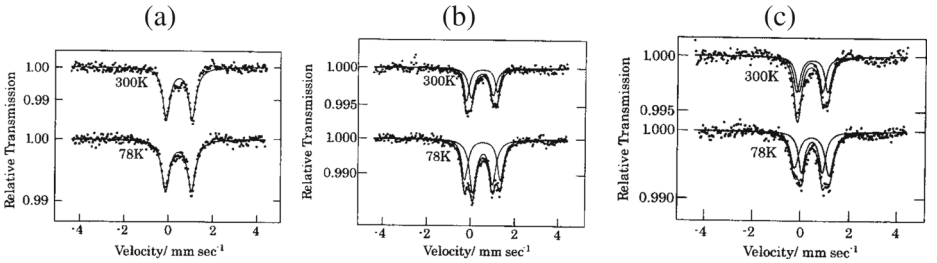

Fig. 1 Variable-temperature ^{57}Fe Mössbauer spectra of (**a**) (*R*, *S*) pentaiodide salt, (**b**) (*R*, *R*) pentaiodide salt, (**c**) (*S*, *S*) pentaiodide salt [3]

property between Mössbauer atom and ligand. Quadrupole splitting (QS) shows the deviation from spherical symmetry in electron distribution. We can easily investigate the valence state and spin state from IS and QS. Furthermore, we can investigate magnetic field from magnetic splitting and we can investigate lattice dynamics from the temperature dependence of the intensity of resonance absorbance. Chemists use Mössbauer spectroscopy to determine the oxidation states, spin states, relative contributions of different iron phases, etc. In the present review, the chemistry concerning mixed-valence state, spin-crossover phenomena, and the chemistry of f-block elements are shown by using Mössbauer spectroscopy combined with X-ray structural analysis and DFT calculation.

2 Mixed-valence states of binuclear metallocenes

Biferrocene derivatives are easily monooxidized to become mixed-valence compounds [2]. Mixed-valence state is interesting, because the new property appears as well as that for each valence state depending on the interaction between the metal ions. If the electron transfer is slow, Fe(II) and Fe(III) can be distinguished. If the electron transfer is fast, valence state becomes detrapped. There are many studies concerning mixed-valence state of biferrocene derivatives. Such mixed-valence state is controlled by the effect of cation symmetry and packing effect. To know such effect, we introduced chiral substituent [3, 4]. We synthesized 1′,1‴-bis(2-phenylbutyl)-1,1″-biferrocenium pentaiodide. 2-Phenylbutyl substituent has *R* and *S* isomer. *R* means clockwise substituent, and *S* means anti-clockwise substituent. We synthesized *R*-*S*, *R*-*R*, and *S*-*S* complexes. *R*-*S* complex has inversion center, while *R*-*R* complex and *S*-*S* complex have never inversion center.

Mössbauer spectroscopy revealed that symmetric *R*-*S* complex shows a valence-detrapped state, while *R*-*R* and *S*-*S* complexes show trapped Fe(II)-Fe(III) state (Fig. 1). X-ray structural analysis revealed that four counter anion zig-zag chains form a symmetric space (Fig. 2). In this symmetric space, mixed-valence monocation is introduced. When the symmetric *R*-*S* complex is introduced, the detrapped valence state is observed. On the other hand, when *R*-*R* complex is introduced, the one *R* substituent (*R*′ substituent) is required to jam into the space. And when *S*-*S* complex are introduced, the one *S* substituent (*S*′ substituent) is required to jam into the space. As the structures of the two ferrocene units differ from each other, the valence state becomes trapped as a result. And the racemic modification consisting of the *R*-*R* and the *S*-*S* isomers showed a perfect detrapped valence state at room temperature, revealing that the packing effect overcomes the effect of cation

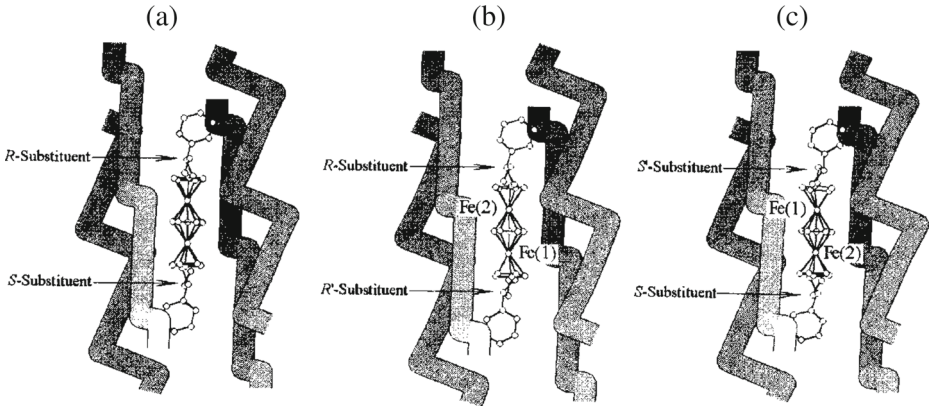

Fig. 2 Illustrated drawing for the cation and its surrounding anion chains: (**a**) the (*R*, *S*) cation; (**b**) the (*R*, *R*) cation; (**c**) the (*S*, *S*) cation [3]

asymmetry. These results show that Mössbauer spectroscopy with X-ray structural analysis has a very important role to understand mixed-valence state.

Ruthenium and osmium are congener element with iron atom. Therefore, the similar mixed-valence complexes with biferrocene derivative are expected for ruthenium and osmium derivatives. Ru(II)-Ru(IV) mixed-valence state was reported where halogen atom is an adduct to Ru(IV) [5]. Recently we synthesized Os(II)-Os(IV) mixed-valence osmium derivative [6, 7]. Halogen atom is also an adduct to Os(IV).

The ^{99}Ru and ^{189}Os Mössbauer spectroscopy cannot easily be applied to the corresponding mixed-valence complexes. Instead, we measured variable-temperature ^{1}H NMR spectra for Os(II)-Os(IV) complex in the solution state. At low temperature, six signals are observed. The three signals (4.86, 5.26, 5.34 ppm) are from Os(II) moiety, and the other three signals (5.48, 5.74, 5.80 ppm) are from Os(IV) moiety. With increasing temperature, six signals are collapsed and then new three peaks appear at the average position between Os(II) and Os(IV). This shows valence-detrapping with increasing temperature. We are now applying DFT calculation to understand the mechanism of the valence detrapping [8].

3 Spin-crossover phenomena for the assembled coordination polymers

If the bridging ligand is used for the synthesis of coordination complexes, metal and ligand are repeated in the crystal, forming an assembled coordination complex. In such situation, there appears a vacancy. This is called porous assembled complex. Many chemists are interested in porous assembled complexes. One of the excellent examples is the gas adsorption [9]. The interest of the coordination polymers for us is whether we can control the spin state of metal by adsorbing or desorbing guest molecule to the vacancy.

There are many studies concerning spin-crossover (SCO) phenomenon for the assembled complexes. We used 1,2-bis(4-pyridyl)ethane (bpa) as bridging ligand [10, 11]. This ligand has *anti* and *gauche* conformer. Depending on these conformers, there are several types of assembled structures. Interpenetrated structure and 2D grid structure can be obtained from *anti* form, while 1D chain structure is obtained from *gauche* conformer. The assembled structures also depend on the anionic ligand and guest molecule. Many enclathrated

complexes showed color change by decreasing temperature. At room temperature the color is pale yellow, while the color becomes deep red by cooling with liquid nitrogen. Such color change is due to the change of spin state.

When the bpa complex has no guest molecule, the spin state remains Fe(II) high spin (HS) state even at low temperature, while guest molecule is introduced, the spin state becomes Fe(II) low spin (LS) state at low temperature, i.e., SCO occurs. The transition temperature changes depending on anionic ligand. Such change is chased by using Mössbauer spectroscopy. At room temperature, IS value is about 1 mm s^{-1}, showing Fe(II) HS state. At low temperature IS is reduced and the singlet is observed, which shows Fe(II) LS state. The HS state has different QS value at room temperature depending on the complex. We plotted the relation between QS value at room temperature and SCO transition temperature obtained by magnetic susceptibility measurements. When the QS value is small, the transition temperature increases [12]. This means that Fe(II) HS state prefers unsymmetrical structure.

1,3-Bis(4-pyridyl)propane (bpp) has one more methylene compared with bpa. There are more variety of conformers. We obtained single crystal using diffusion method [13, 14]. Usually guest-free complex is obtained. However, when we use benzene as solvent, benzene-enclathrated complex is obtained. Guest-free complex shows an interesting 2D interpenetrated structure, while benzene-enclathrated complex shows 1D chain structure.

Powder X-ray diffraction patterns revealed a structural change accompanied by sorption of benzene molecule. By desorbing the benzene molecule from $Fe(NCBH_3)_2(bpp)_2 \cdot 2(benzene)$, the pattern is changed. The pattern for the desorbed one is very similar to that for 2D interpenetrated one. And then, by re-adsorbing benzene molecule, the pattern returned to the original pattern.

Magnetic susceptibility measurement of $Fe(NCBH_3)_2(bpp)_2$ revealed that benzene-enclathrated complex shows SCO-off state. SCO-off means that Fe(II) HS state is observed at all temperatures. By desorbing benzene molecule from $Fe(NCBH_3)_2(bpp)_2 \cdot 2(benzene)$, SCO occurs, which is SCO-on system. And then by re-adsorbing benzene molecule, it returns to SCO-off state. We can chase such change by using Mössbauer spectra. Benzene-enclathrated sample shows SCO-off state, by desorbing benzene molecule, IS and QS change, and readsorbing benzene molecule, the IS and QS values become the same with original values.

Hitherto, we introduced the results for bpa complexes and bpp complexes. In bpa complexes, SCO is off in the guest-free complexes, and SCO is on when the complex includes guest molecule. On the other hand, in bpp complexes, SCO is on in the guest-free complexes, and SCO is off when the complex includes guest molecules. There appeared an opposite effect of guest molecule between bpa complex and bpp complex. Question is what the role of guest molecule is. It is said that the weak intermolecular interaction is important for the appearance of SCO. What determines the spin state? We performed DFT calculation to answer the question.

We checked our crystal data. There are many papers for the assembled coordination polymers using other bridging ligand. We also checked the structure in the literature [15–19]. We noticed the importance of local structure around iron atom. Local structures around iron atom are classified into propeller type, parallel type, and distorted propeller type (Fig. 3). When the local structure is propeller type, SCO occurs. On the other hand, the local structure is parallel or distorted propeller, SCO is off. We studied whether such kind of difference in local structure around iron atom affects spin state or not. We performed DFT calculation by using ORCA [20]. We used mono-nucleus model for the calculation [21, 22]. We cut out the part of $Fe(NCS)_2py_4$ from X-ray coordinate.

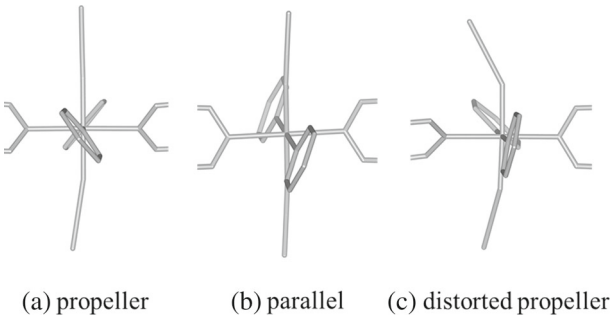

Fig. 3 Local structures for $[Fe(NCS)_2L_2]$ coordination polymers

Geometry optimization and vibrational frequency analysis were performed using BP86 functional. We constructed dihedral angle between Py and axial NCS. Single point calculation was performed using several functional such as BP86 etc. BP86, PBE, TPSS are pure DFT, while PBE0, B3LYP, B3LYP*, TPSSh are hybrid-DFT. By changing the functional, the rate of Hatree-Fock exchange admixture changes. By such change, relative stability changes between HS state and low LS state.

Zero-point corrected energy (E_0) is estimated by the sum of total energy (E_{tot}) obtained by TPSSh single-point calculation and zero-point energy obtained by BP86 vibrational frequency calculation. Zero-point corrected energy difference ($\Delta E_0^{\mathrm{HL}} = E_0^{\mathrm{HS}} - E_0^{\mathrm{LS}}$) becomes an indicator for predicting whether SCO occurs or not. If the value is negative, SCO becomes off. On the other hand, when the value is positive, SCO appears. We can judge whether SCO occurs or not by using the sign. By comparing the calculation results with experimental results, it was found that TPSSh functional is the best.

Spin transition curve can be obtained by considering Gibbs energy change under adiabatic condition. And we treated these systems as the condition of no intermolecular-interaction (1). Because the SCO-on/off is basically determined by the ligand field strength and the intermolecular interaction affects the hysteresis.

$$\gamma_{\mathrm{HS}}(T) = [1 + \exp(\Delta G^{\mathrm{HL}}/k_{\mathrm{B}}T)]^{-1} \tag{1}$$

Spin transition curve by calculation reproduces excellently the experiment behavior.

We checked the role of dihedral angle. We fixed the dihedral angle between two pyridine ligands across iron atom 60°. And we changed the dihedral angle between pyridine and NCS from 30° to 60° (Fig. 4). When the dihedral angle is 30°, the LS state is more stable, in this case SCO occurs, by increasing the angle, the LS state becomes unstable drastically compared with HS state (Fig. 5). In this case SCO does not occur. This reveals that the dihedral angle is a key to determine whether SCO occurs or not. This means that ligand has to approach metal to become LS state, but in distorted structure, it becomes difficult by steric hindrance.

The d-orbital splitting for both spin states shows the pseudo tetragonal symmetric field shrinking along Fe-NCS axis. Defining the average energy (ε) of each t_{2g} and e_g orbital as the summation weighted by the fraction of d-orbital belonging to each orbital region (ω_i), we estimated the ligand field splitting (Δ_{o}) by employing next equation (2).

$$\Delta_{\mathrm{o}} = \varepsilon(\mathrm{e_g}) - \varepsilon(\mathrm{t_{2g}}) = \Sigma_i \omega_i(\mathrm{e_g})\varepsilon_i(\mathrm{e_g}) - \Sigma_i \omega_i(\mathrm{t_{2g}})\varepsilon_i(\mathrm{t_{2g}}) \tag{2}$$

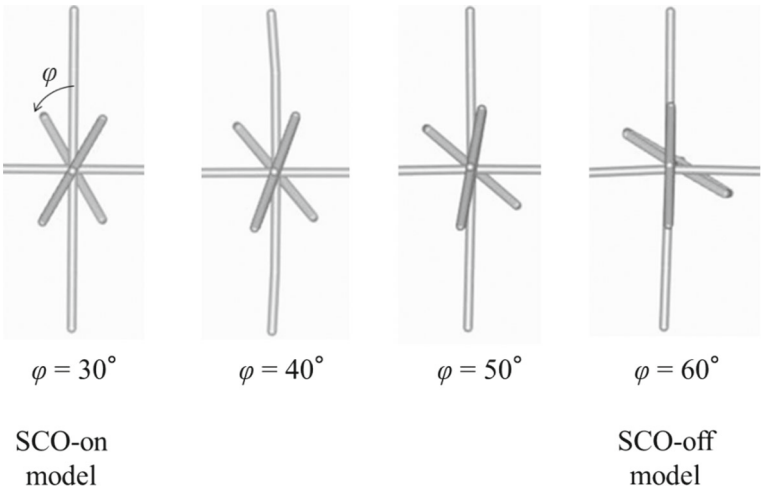

Fig. 4 Models of SCO-on ⇒ SCO-off [21]

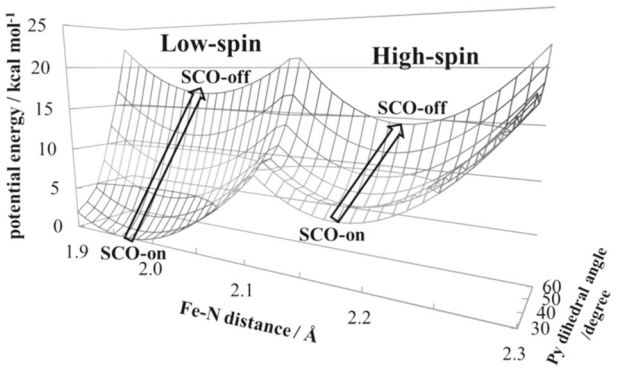

Fig. 5 Potential energy surface of Fe-N and pyridine dihedral angle [21]

Good correlation with ΔE_0^{HL} is not obtained for $\Delta_{\mathrm{o}}^{\mathrm{HS}}$ of both α- and β-spin orbitals. On the other hand, Δ_{o} values of LS correlate well with ΔE_0^{HL}. This result implies that the variation of ΔE_0^{HL}, which is a crucial parameter for SCO behavior, depends on the change of $\Delta_{\mathrm{o}}^{\mathrm{LS}}$. Although, it is not new that the ligand field splitting contributes to the ΔE_0^{HL}, as possible as we know, the detailed estimation of Δ_{o} for SCO compounds by means of DFT calculation has never discussed. Furthermore, regarding $\Delta_{\mathrm{o}}^{\mathrm{LS}}$ values as the meaningful parameter for the prediction of SCO-on/off behavior, the analogous plotting to Tanabe-Sugano diagram based on the obtained data is examined. This diagram was plotted as the function of $\Delta_{\mathrm{o}}^{\mathrm{LS}}$ versus the relative zero-point corrected energy to the most stable spin state. The crossing point of the ligand field splitting of LS is obtained where ΔE_0^{HL} is zero as ∼4.61 eV.

It has been said that the weak intermolecular interaction is important to control spin state. This is explained from the present result as follows. Weak interaction between ligands or

the interaction with guest molecule controls the local structure around iron atom. Such local structure determines the SCO-on/off, when the ligand field is intermediate. Of course, if the intermolecular interaction becomes larger, hysteresis will be expected.

4 Benchmark study for the separation of Ln/MA

The study of separation of minor actinide (MA) from lanthanide (Ln) is important from the two points. One is from the point of application to the field of nuclear power engineering. MA has long life time and harmful radiation. Separation of MA from Ln in high-level wastes is needed. The other is from the point of basic chemistry of f-elements. Ln has 4f electron and MA has 5f electron. What is the chemical difference between Ln and MA? We would like to know the difference in bonding character between 4f and 5f.

Solvent extraction using ligand is used for the separation. There are many reports for the separation of Eu and Am. Distribution coefficient from water phase to organic phase can be obtained for Eu and Am. Separation factor is obtained by the ratio of the two distribution coefficients. This separation factor depends on donor atom. In the case of S donor and N donor, there is a good selectivity to Am, while in the case of O donor, there is a good selectivity to Eu. What kind of bonding character affects such difference between Ln and MA?

We started the study using DFT calculation. What kind of method is adequate or not is an important problem in the calculation. To know this, we performed benchmark study by using Mössbauer isomer shift of ^{151}Eu and ^{237}Np [23]. The connection of Mössbauer isomer shift with DFT can be achieved by the linear relationship between δ and ρ_0 values (3)

$$\delta^{\mathrm{exp}} = a(\rho_0^{\mathrm{calc}} - b) \tag{3}$$

where δ^{exp} and ρ_0^{calc} are the experimental δ value and the calculated ρ_0 value for the target compounds, respectively, a and b are the constants fitted by the relationship between δ^{exp} and ρ_0^{calc}.

We performed DFT calculation by using ORCA [20]. Scalar-relativistic correction was considered by zeroth-order regular approximation (ZORA) Hamiltonian including atomic model potential, which was modified by s-type Gaussian atomic density. All-electron Gaussian-type orbitals were employed as basis functions in all SCF calculations. The calculation of Mössbauer parameters unconditionally requires all-electron basis set since it needs the information of the electron density at the nucleus position. In the case of actinide, Mössbauer data of ^{237}Np can be used. We performed benchmark study of ^{151}Eu and ^{237}Np instead of Am. It was shown that B2PLYP is the best method.

We performed the separation study on Eu(III) / Am(III) ions with S-, N- and O-donor ligands by means of scalar-relativistic ZORA-DFT calculation [24]. We considered the complex formation reactions in which the chemical components and geometries were experimentally confirmed. The equilibrium structures at ZORA-BP86 / SARC level were consistent with the experimental structures. As the results of the single-point calculations by BP86, B3LYP and B2PLYP functionals, the reproducibility of the selectivity of Eu(III) / Am(III) was increased in order of BP86, B3LYP and B2PLYP functionals, especially B2PLYP functional also reproduced the absolute values of $\Delta\Delta G(= \Delta G_{\mathrm{Eu}} - \Delta G_{\mathrm{Am}})$. This tendency of the reproducibility was consistent with that of ^{151}Eu and ^{237}Np Mössbauer isomer shifts, indicating that the method which can describe the accurate bonding nature in compounds is required to reproduce the experimental selectivity of Eu(III) / Am(III). The results of Mulliken's spin population suggested that BP86 and B3LYP overestimated

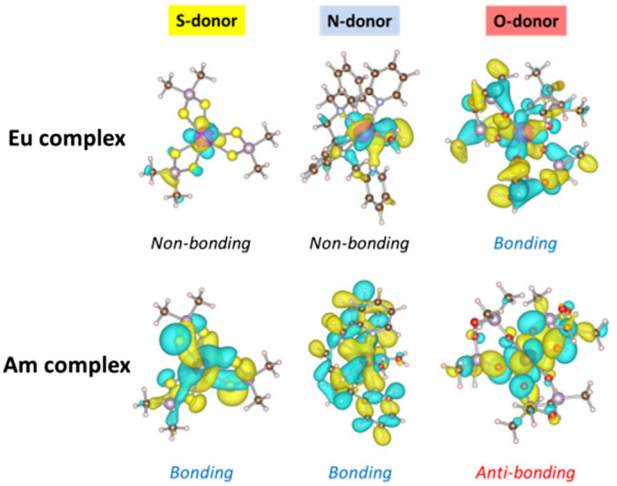

Fig. 6 The difference in the bonding types in f-orbital between Eu(III) and Am(III) complexes depending on S-, N- and O-donor ligands [24]

the covalency in the bonding of Eu-ligand compared to that of Am-ligand, leading to the inconsistency of $\Delta\Delta G$. Bond overlap population analysis at B2PLYP level revealed that the bonding property between f-orbital of Eu and donor atoms was basically ionic, whereas the strong covalent interaction was observed in the f-orbital of Am. Furthermore, the bonding types of Am f-orbital were "bonding" in S- and N-donor complexes, but "anti-bonding" in O-donor complex, resulting in the difference in whether donor atoms favor Am ion or not (Fig. 6). We first explained comprehensively the origin of Eu(III) / Am(III) selectivity by the difference in the contribution of f-electron to the bonding between metal and donor atoms. It might be expected that our calculation procedure contributes to the prediction of Eu(III) / Am(III) selectivity and the improvement of the separation materials based on the chemical bonding properties between f-orbital and ligands by the molecular modification and/or the element strategy.

5 Conclusion

Mössbauer spectroscopy combined with X-ray structural analysis and DFT calculation reveals the nature of mixed-valence state of binuclear metalloenes and SCO phenomena in the assembled coordination polymers. Benchmark study between δ^{exp} and ρ_0^{calc} obtained by DFT calculation reveals which functional is the best to understand experimental results. By using this result the difference in the separation of Eu and Am is revealed from the chemical bonding between 4f and 5f and their S-, N-, and O-donor ligands.

Acknowledgements This is the work by our research group. Especially, we thank Dr. Oda, Mr. Morita, Mr. Atsuchi, Dr. Yasuhara, Dr. Kaneko, and Dr. Miyashita.

References

1. Gütlich, P., Link, R., Trautwein, A.: Mössbauer Spectroscopy and Transition Metal Chemistry. Springer, Heidelberg (1978)
2. Hendrickson, D.N.: Electron Transfer in Mixed-Valence Complexes in the Solid State, in Mixed valency Systems: Applications in Chemistry, Physics and Biology. Kluwer, Dordrecht (1991)
3. Oda, T., Okuda, T., Nakashima, S.: Mixed-valence state of optically active 1′,1‴-Bis(2-phenylbutyl)-1,1″-biferrocenium penraiodide: effects of cation symmetry and intermolecular interaction on trapped-/detarpped-valence states. Inorg. Chem. **42**, 5376–5383 (2003)
4. Oda, T., Okuda, T., Nakashima, S.: Mixed-valence states of 1′,1‴-Bis(2-phenylbutyl)-1,1″-biferrocenium(1+) triiodides: effects of the cation symmetry and counter anion on the electron-transfer rate. Bull. Chem. Soc. Jpn. **76**, 2129–2134 (2003)
5. Watanabe, M., Iwamoto, T., Kawata, S., Kubo, A., Sano, H., Motoyama, I.: Carbon-13 CP-MAS, carbon-13 and proton NMR spectroscopic study of mixed-valence 1,1″-biruthenocenium salts. Inorg. Chem. **31**, 177–182 (1992)
6. Yasuhara, H., Koga, K., Nakashima, S.: Synthesis and oxidation study of the simplest binuclear metallocene compound of osmium, biosmocene. J. Organomet. Chem. **779**, 86–90 (2015)
7. Yasuhara, H., Nakashima, S.: Halogen effect on mixed-valence state of biosmocenium(II, IV) salts. J. Organomet. Chem. **791**, 225–231 (2015)
8. Kaneko, M., Yasuhara, H., Miyashita, S., Nakashima, S., unpublished results.
9. Kitagawa, S., Matsuda, R.: Chemistry of coordination space of porous coordination polymers. Coord. Chem. Rev. **251**, 2490–2509 (2007)
10. Morita, T., Asada, Y., Okuda, T., Nakashima, S.: Isomerism of assembled iron complex bridged by 1,2-di(4-pyridyl)ethane and its solid-to-solid transformation accompanied by a change of electronic state. Bull. Chem. Soc. Jpn. **79**, 738–744 (2006)
11. Morita, T., Nakashima, S., Yamada, K., Inoue, K.: Occurrence of the spin-crossover phenomena of assembled complexes, $Fe(bpa)_2(NCX)_2$ (bpa=1,2-bis(4-pyridyl)ethane; X=S, BH_3) by enclathrating organic guest molecule. Chem. Lett. **35**, 1042–1043 (2006)
12. Nakashima, S., Morita, T., Inoue, K.: Spin-crossover phenomenon of the assembled iron complexes with 1,2-bis(4-pyridyl)ethane as bridging ligand studied by Mössbauer spectroscopy. Hyperfine Interact. **188**, 107–111 (2009)
13. Atsuchi, M., Higashikawa, H., Yoshida, Y., Nakashima, S., Inoue, K.: Novel 2D interpenetrated structure and occurrence of the spin-crossover phenomena of assembled complexes, $Fe(NCX)_2(bpp)_2$ (X = S, Se, BH_3; bpp = 1,3-Bis(4-pyridyl)propane. Chem. Lett. **36**, 1064–1065 (2007)
14. Atsuchi, M., Inoue, K., Nakashima, S.: Reversible structural change of host framework triggered by desorption and adsorption of guest benzene molecules in $Fe(NCS)_2(bpp)_2 \cdot 2$(benzene) (bpp = 1,3-bis(4-pyridyl)propane). Inorg. Chim. Acta **370**, 82–88 (2011)
15. Real, J.A., Andrés, E., Muñoz, M.C., Julve, M., Granier, T., Bousseksou, A., Varret, F.: Spin crossover in a catenane supramolecular system. Science **268**, 265–267 (1995)
16. Moliner, N., Muñoz, C., Létard, S., Solans, X., Menéndez, N., Goujon, A., Varret, F., Real, J.A.: Spin crossover bistability in three mutually perpendicular interpenetrated (4,4) nets. Inorg. Chem. **39**, 5390–5393 (2000)
17. Neville, S.M., Halder, G.J., Chapman, K.W., Duriska, M.B., Moubaraki, M., Murray, K.S., Kepert, C.J.: Guest tunable structure and spin crossover properties in a nanoporous coordination framework material. J. Am. Soc. Chem. **131**, 12106–12108 (2009)
18. Halder, G.J., Kepert, C.J., Moubaraki, B., Murray, K.S., Cashion, J.D.: Guest-dependent spin crossover in a nanoporous molecular framework material. Science **298**, 1762–1765 (2002)
19. Halder, G.J., Chapman, K.W., Neville, S.M., Moubaraki, B., Murray, K.S., Létard, J., Kepert, C.J.: Elucidating the mechanism of a two-step spin transition in a nanoporous metal–organic framework. J. Am. Chem. Soc. **130**, 17552–17562 (2008)
20. Neese, F.: ORCA-an ab initio, density functional and semiempirical program package, version 2.8, 2008 (http://www.thch.uni-bonn.de/tc/orca/)
21. Kaneko, M., Tokinobu, S., Nakashima, S.: Density functional study on spin-crossover phenomena of assembled complexes, $[Fe(NCX)_2(bpa)_2]_n$ (X = S, Se, BH_3; bpa = 1,2-bis(4-pyridyl)ethane). Chem. Lett. **42**, 1432–1434 (2013)
22. Kaneko, M., Nakashima, S.: Computational study on thermal spin-crossover behavior for coordination polymers possessing trans-$Fe(NCS)_2$(pyridine)$_4$ unit. Bull. Chem. Soc. Jpn. **88**, 1164–1170 (2015)

23. Kaneko, M., Miyashita, S., Nakashima, S.: Benchmark study of Mössbauer isomer shifts of Eu and Np complexes by relativistic DFT calculation for the understanding of bonding nature of f-block compounds. Dalton Trans. **44**, 8080–8088 (2015)
24. Kaneko, M., Miyashita, S., Nakashima, S.: Bonding study on the chemical separation of Am(III) from Eu(III) by S-, N- and O-donor ligands by means of all-electron ZORA-DFT calculation. Inorg. Chem. **54**, 7103–7109 (2015)